Charge Density Study of the Polymorphs of *p*-Nitrophenol

G. U. Kulkarni, P. Kumaradhas, and C. N. R. Rao*

Chemistry and Physics of Materials Unit, Jawaharlal Nehru Centre for Advanced Scientific Research, Jakkur, Bangalore 560 064, India

Received April 13, 1998. Revised Manuscript Received July 27, 1998

A careful investigation of the structures and charge densities of the β and α polymorphs of *p*-nitrophenol has been carried out. Although the two forms crystallize in different monoclinic cells, the crystal densities are similar. There are, however, several differences in the intramolecular structural features of the two forms, including the C−C−O bond angles and the N−O distances. The α form exhibits a large number of intermolecular hydrogen contacts. More importantly, a detailed charge density analysis of the two forms has brought out significant differences in the charge distribution in both the intra- and the intermolecular hydrogen bonding regions. Deformation density maps reveal many differences in the bonding regions of the molecule in the two forms. Charge migration from the benzene ring region of the molecule to the nitro and the hydroxyl groups occurs as the structure changes from the β to the α form. Relief maps of the negative Laplacians in the plane of the intermolecular hydrogen bonds show polarization of the oxygen lone-pair electrons toward hydrogen. The molecular dipole moments in the solid state, derived from the pseudoatomic charges in the β and α structures, are considerably larger (∼20 D) than the value in the free molecule.

Introduction

Polymorphism in molecular organic crystals is ubiquitous.[1] Depending on the conditions of crystallization, molecules adopt different strategies of packing, giving rise to different crystal structures, often incorporating minor changes in the molecular structure itself. Among the different polymorphs of a substance, there are only small differences in the free energy, approximately a few kilocalories per mole at most; the transformation from the thermodynamically unstable form to the stable one commonly occurs through displacive movements of the molecules.[2] *p*-Nitrophenol exhibits polymorphism where one of the polymorphs is light sensitive. The α form of the *p*-nitrophenol, which crystallizes from ether or benzene solution, undergoes a topochemically controlled photochemical transformation, manifesting itself in an irreversible color change of the solid from yellow to red. On the other hand, the β modification, which can be crystallized from aqueous solution, is light stable at room temperature and transforms to the α form on mild heating. Thus, *p*-nitrophenol provides an interesting example of polymorphism where one polymorph is thermodynamically unstable and the other is photochemically unstable. Some years ago, Coppens and Schmidt[3,4] carried out a study of the crystal structures of the β and α forms and concluded that the stable α form has a relatively greater number of close contacts. In order to explain the photochemical activity, they proposed a redox reaction along the intermolecular CH···ON contacts. We considered the *p*-nitrophenol system to be of sufficient interest to carry out a charge density study. Such a study was expected to show differences in the charge densities of the two polymorphic forms, which could bestow different chemical reactivities in them. It was also our feeling that this system would be a good starting point for our efforts in investigating charge densities of organic crystals in relation to chemical reactivity and dependence on the polymorphic form. Furthermore, *p*-nitrophenol is a good model compound with push−pull electron interaction analogous to that in nonlinear materials and other intramolecular charge-transfer systems.

The experimental charge density method to study intra- and intermolecular bonding in molecular crystals has become popular and powerful in recent years with the advent of area detectors and the well-seasoned multipole formalism.[5,6] For instance, Cameron and his co-workers[7] have examined charge densities in aziridinyl, benzene, and phosphozene rings experimentally and compared them with the theory. Iwasaki et al.[8] carried out deformation density measurements to understand the nature of hypervalent S···N bonds. Charge density analysis of the hydrogen bonds in maleate salts have been reported recently.[9,10] There have been studies on

(1) Dunitz, J. D. *Pure Appl. Chem*. **1991**, *63*, 177.
(2) Rao, C. N. R. *J. Mol. Struct*. **1993**, *292*, 229.
(3) Coppens, P.; Schmidt, G. M. J. *Acta Crystallogr*. **1965**, *18*, 654.
(4) Coppens, P.; Schmidt, G. M. J. *Acta Crystallogr*. **1964**, *17*, 222.
(5) Coppens, P. *J. Phys. Chem*. **1989**, *93*, 7979. Coppens, P. *X-ray charge densities and chemical bonding*; Oxford University Press: New York, 1997.
(6) Jeffrey, G. A., Piniella, J. F., Eds. *The Application of Charge Density Research to Chemistry and Drug Design*; Plenum Press: New York, 1991.
(7) Cameron, T. S.; Borecka, B.; Kwiatkowski, W. *J. Am. Chem. Soc*. **1994**, *116*, 1211.
(8) Iwasaki, F.; Yoshida, S.; Kakuma, S.; Watanabi, T.; Yasui, M. *J. Mol. Struct*. **1995**, *352/353*, 203.
(9) Mallinson, P. R.; Wozniak, K.; Garry, T.; McCormack, K. L. *J. Am. Chem. Soc*. **1997**, *119*, 11502.

10.1021/cm980277m CCC: $15.00
Published on Web 10/17/1998

inorganic complexes as well. The deformation around the nickel atom in tetragonal $NiSO_4 \cdot 6H_2O$ has been shown to be similar to that predicted by the crystal field theory.[11] Henaff et al.[12] have analyzed the deformation density in LiB_3O_5 in terms of σ and π bonding. The charge density method is also gaining importance in medicinal research. Potential drug molecules such as L-Dopa have been investigated.[13] Charge density studies on vitamin C[14] and DL-aspartic acid[15] have been reported recently. Some workers have analyzed non-centrosymmetric crystals of importance in nonlinear optics.[16,17] In the present study, we have carried a detailed investigation on the β and α polymorphs of *p*-nitrophenol using the charge density method, having collected high-resolution X-ray diffraction data at low temperatures on both forms as well as on the irradiated crystal of the α form. Our study has shown differences in the molecular structure in the β and α forms, particularly in the hydrogen bond region and, more importantly, significant differences in the charge densities and associated properties of the two forms. It is noteworthy that molecular dipole moments of *p*-nitrophenol in the solid state turns out to be ∼20 D, much larger than that of the free molecule. Such charge density studies of polymorphs of a substance would be of relevance in understanding intramolecular charge transfer in molecular materials.

Experimental Section

Pale yellow crystals of the β and α forms were grown from the aqueous and the benzene solutions, respectively. High-quality crystals of the two modifications were chosen after detailed examination under an optical microscope. X-ray diffraction intensities were measured by ω scans using Siemens three-circle diffractometer attached with a CCD area detector and a graphite monochromator for the Mo Kα radiation (50 kV, 40 mA). The crystals were cooled on the diffractometer using a stream of cold nitrogen gas from a vertical nozzle and were held at 110 K throughout the data collection. Extra care was taken not to expose the α crystal to light for extended hours during the experiment.

Initially the unit cell parameters and the orientation matrix of the crystal were determined using ∼60 reflections from 25 frames collected over a small ω scan of 7.5°. A hemisphere of reciprocal space was then collected in two shells using SMART software[18] with 2θ settings of the detector at 32 and 70°. The coverage was found to be ∼92% using the ASTRO routine.[18] The data reduction was performed using the SAINT program,[18] and the orientation matrix and the detector and the cell parameters were refined for every 40 frames on all of the measured reflections. The experimental details are listed in Table 1. As a preliminary check on the X-ray intensity data, the crystal structures of the polymorphs were redetermined using the SHELXTL program[19] and were compared with the reported structures.

As a first step toward charge density analysis, a high-order refinement of the data was carried out using reflections with $\sin\theta/\lambda \geq 0.85$ Å^{-1} and $F_o \geq 10\sigma$. The H atom positions were found using the difference Fourier method and were adjusted to theoretical values (C−H, 1.085 Å; O−H, 0.96 Å) and were held constant throughout the refinement along with their isotropic temperature factors. As usual, the non-hydrogen atoms were treated anisotropically. The results of the refinement are listed in Table 2. These served as the initial parameters for the multipolar refinement.

Multipolar refinement for the charge density analysis was carried out using the XDLSM routine of the XD package.[20] The non-hydrogen atoms were refined up to the octapole moments, while the hydrogen atoms were restricted to the quadrupole moments. Charge neutrality constraint was applied to the molecule through all cycles of refinement. The *r*-factors showed significant improvement over the conventional refinement from around 6% to ∼2%. The κ refinement was also carried out, and following that, the residual index showed marginal improvement. The XDPROP routine was used to calculate the total electron density $\rho(r)$, the deformation density $\Delta\rho$, and the Laplacian $\nabla^2\rho$. These results are listed in Table 3.

Charge density analysis of the intermolecular hydrogen contacts was carried out using the PARST[21] and XD programs, and the results are given in Table 4. Pseudoatomic charges and the dipole moments obtained using XDPROP are listed in Table 5.

Results and Discussion

Structures of the β and α Forms. In Figures 1 and 2 we show the molecular packing diagrams of the β and α forms, respectively. The molecular structure differs in the two forms to some extent. A look at the torsion angles, listed in Table 2, suggests that the OH and the NO_2 groups are not coplanar with the benzene rings in both forms, the constituent atoms of the two groups showing noticeable displacements above and below the mean plane of the benzene ring. In the β form, the N atom remains in the mean plane while the O(3), O(1), and H(1) atoms show small displacements of −0.08, +0.05, and −0.03 Å, respectively. The O(2) atom of the nitro group shows the largest displacement of 0.22 Å from the benzene mean plane. Coppens and Schmidt[3] obtained a value of 0.185 Å for this displacement. In the α form, on the other hand, the H(1) atom of the OH group is maximally displaced from the benzene ring plane (0.32 Å), while the N, O(2), O(3), and O(1) atoms exhibit small displacements of 0.05, 0.04, 0.09, and 0.03 Å, respectively.

The C−C−O bond angles in *p*-nitrophenol are not equal (see Figures 1 and 2), a feature common to many other phenolic compounds. This inequality is considered to be due to the bent orbitals resulting from the repulsion between the hydrogen atom and the carbon carrying the hydroxyl group.[22] We observe some differences between the β and α forms of *p*-nitrophenol in relation to this inequality. The values are 6.24° for the β form and 5.5° for the α form which closely match the values of 6.5 and 5.6° reported by Coppens and

(10) Madsen, D.; Flensburg, C.; Larsen, S. *J. Phys. Chem.* **1998**, *102A*, 2177.
(11) Ptasiewicz-Bak, H.; Olovsson, I.; McIntyre, G. J. *Acta Crystallogr.* **1997**, *B53*, 325.
(12) Henaff, C. L.; Hansen, N. K.; Protas, J.; Marnier, G. *Acta Crystallogr.* **1997**, *B53*, 870.
(13) Howard, S. T.; Hursthouse, M. B.; Lemann, C. W.; Poyner, E. A. *Acta Crystallogr.* **1995**, *B51*, 328.
(14) Milanesio, M.; Bianchi, R.; Ugliengo, P.; Viterbo, D. *THEOCHEM* **1997**, *419*, 139.
(15) Flaig, R.; Koritsanszky, T.; Zobel, D.; Luger, P. *J. Am. Chem. Soc.* **1998**, *120*, 2227.
(16) Hamzaoui, F.; Bret, F.; Wojcik, G. *Acta Crystallogr.* **1996**, *B52*, 159.
(17) Howard, S. T.; Hursthouse, M. B.; Lehmann, C. W.; Mallinson, P. R.; Frampton, C. S. *J. Chem. Phys.* **1992**, *97*, 5616.
(18) Siemens Analytical X-ray Instruments Inc., Madison, WI, 1995.
(19) *SHELXTL* (Silicon graphics version); Siemens Analytical X-ray Instruments Inc.: Madison, WI, 1995.
(20) Koritsansky, T.; Howard, S. T.; Richter, T.; Mallinson, P. R.; Su, Z.; Hansen, N. K. *XD, A computer Program Package for Multipole Refinement and Analysis of Charge Densities from Diffraction Data*; Cardiff, Glasgow, Buffalo, Nancy, 1995.
(21) Naradelli, M. *Comput. Chem.* **1983**, *7*, 95.
(22) Hirshfeld, F. L. *Isr. J. Chem.* **1964**, *2*, 87.

Table 1. Crystal Data and Experimental Details

chem formula	$C_6H_5NO_3$	
fw	139.11	
cell setting	monoclinic	
	β	α
space group	$P2_1/n$	$P2_1/c$
a (Å)	3.6812(3)	6.1664(1)
b (Å)	11.1152(9)	8.8366(3)
c (Å)	14.6449(12)	11.5435(4)
β (deg)	92.804(2)	103.390(1)
D_x (mg m^{-3})	1.544	1.510
radiation type	Mo Kα	
wave length (Å)	0.710 73	
no. of reflecns for cell params	9874	10029
μ (mm^{-1})	0.13	0.12
temp (K)	110	
cryst form	needle	rectangular block
cryst size (mm)	0.4 × 0.32 × 0.28	0.3 × 0.2 × 0.14
cryst color	pale yellow	pale yellow
	Data Collection	
diffractometer	Siemens CCD	
data collection	ω scan	
crystal−detector distance (cm)	4.0	
no. of measrd reflecns	9874	10029
no. of independent reflecns	4603	4147
no. of obsd reflecns	4459	4045
R_{merge}	0.035	0.033
R_{int}	0.035	0.035
θ_{max} (deg)	49.93	49.61
$(\sin\theta/\lambda)_{max}$	1.08	1.07
range of h, k, l	$-7\rightarrow h\rightarrow+7$ $-23\rightarrow k\rightarrow+16$ $-28\rightarrow l\rightarrow+15$	$-10\rightarrow h\rightarrow+11$ $-18\rightarrow k\rightarrow+13$ $-23\rightarrow l\rightarrow+15$
	Refinement (Multipole and κ)	
refinement on F		
R	0.025	0.022
R_w	0.032	0.029
S	1.89	1.80
no. of reflecns used in the refinement	4459	4045
no. of params used	*303*	*303*
N_{ref}/N_v	*14.8*	*13.4*
H-atom treatment	see text	
weighting scheme	$w = 1/\sigma^2(F) = (4F^2)/\sigma^2(F^2)$ $\sigma^2(F^2) = \sigma^2_{counting}(F^2) + P^2(F^4)$	
$(\text{shift/e.s.d})_{max}$	*0.06*	*0.01*
$\Delta\rho_{max}$(e Å^{-3})	*0.12*	*0.07*
$\Delta\rho_{min}$(e Å^{-3})	*−0.10*	*−0.11*

Schmidt.[3,4] The C−C−N bond angles show small differences. Furthermore, the N−O(3) bond is slightly longer by 0.01 Å in the α form, compared to the β form.

The crystal packing in the β and α modifications is noticeably different. The β form crystallizes in the $P2_1/n$ space group, with the cell dimensions of a = 3.6812(3) Å, b = 11.152(9) Å, c = 14.6449(12) Å, and β = 92.804-(2)°. We find no orientational relation of this cell with that of the α form,[23] which occurs in the $P2_1/c$ space group with a = 6.1664(1) Å, b = 8.8366(3) Å, c = 11.5435(4) Å, and β = 103.390(1)°. The densities are comparable to those obtained by Coppens and Schmidt.[3,4] The approach of the adjacent molecules is obviously different in the two structures. The adjacent nonparallel molecules subtend an angle of 74.73° in the α form, but they tend to align nearly parallelly in the β form (29.26°). Similar values (∼74 and 28°) have been reported earlier.[3,4]

The differences in the crystal packing between the β and α forms are reflected in the intermolecular hydrogen bonds (see Figures 1 and 2 as well as Table 4). In the β structure, there are two nearly parallel H-bonds originating from the nitrooxygens apart from the four other bonds involving the phenyl hydrogens. In the α form, as many as nine hydrogen contacts can be predicted. In both forms, the O(3)···H(1) contact at ∼1.9 Å, with an O(3)···H(1)−O(1) angle greater than 160°, appears to be the strongest. It is interesting that H(1) interacts with the entire nitro group in the α structure, and it is possible that the stability of the α structure is related to such favorable hydrogen bonding in the intermolecular region. Charge density analysis throws light on this aspect as will be seen later.

Charge Density Analysis. The model of refinement used by us is based on a promolecular density obtained as a superposition of the spherical atomic densities centered at the nuclear positions. The promolecule can serve as a reference state relative to which charge migration due to bond formation takes place. In order to visualize the charge distribution due to the chemical bond formation, a refinement formalism based on the nucleus-centered multipole expansion of the electron

(23) Cohen, M. D.; Coppens, P.; Schmidt, G. M. J. *J. Phys. Chem. Solids* **1964**, *25*, 258.

Table 2. Bond Lengths and Angles from High-Order Refinement

	β	α
Bond Lengths (Å)		
C(1)−C(2)	1.402(1)	1.411(1)
C(1)−C(6)	1.405(1)	1.408(1)
C(1)−O(1)	1.349(1)	1.359(1)
C(2)−C(3)	1.391(1)	1.392(1)
C(2)−H(2)	1.085	1.085
C(3)−C(4)	1.395(1)	1.402(1)
C(3)−H(3)	1.085	1.085
C(4)−C(5)	1.396(1)	1.403(1)
C(4)−N	1.447(1)	1.452(1)
C(5)−C(6)	1.384(1)	1.391(1)
C(5)−H(5)	1.085	1.085
C(6)−H(6)	1.085	1.085
O(1)−H(1)	0.96	0.96
O(2)−N	1.235(1)	1.237(1)
O(3)−N	1.238(1)	1.251(1)
Bond Angles (deg)		
C(6)−C(1)−O(1)	116.8(1)	117.1(1)
C(2)−C(1)−O(1)	123.1(1)	122.6(1)
C(2)−C(1)−C(6)	120.1(1)	120.3(1)
C(1)−C(2)−H(2)	120.0(1)	120.1(1)
C(1)−C(2)−C(3)	120.1(1)	119.9(1)
C(3)−C(2)−H(2)	120.0(1)	120.1(1)
C(2)−C(3)−H(3)	120.6(1)	120.6(1)
C(2)−C(3)−C(4)	118.7(1)	118.9(1)
C(4)−C(3)−H(3)	120.6(1)	120.6(7)
C(3)−C(4)−N	119.2(1)	119.6(1)
C(3)−C(4)−C(5)	122.0(1)	122.1(1)
C(5)−C(4)−N	118.8(1)	118.4(1)
C(4)−C(5)−H(5)	120.6(1)	120.6(1)
C(4)−C(5)−C(6)	118.9(1)	118.7(1)
C(6)−C(5)−H(5)	120.6(1)	120.6(1)
C(1)−C(6)−C(5)	120.2(1)	120.1(1)
C(5)−C(6)−H(6)	119.9(1)	120.0(1)
C(1)−C(6)−H(6)	119.9(1)	120.0(1)
C(1)−O(1)−H(1)	109.5(1)	109.5(1)
O(2)−N−O(3)	122.6(1)	122.3(1)
C(4)−N−O(3)	118.8(1)	118.5(1)
C(4)−N−O(2)	118.6(1)	119.3(1)
Torsion Angles (deg)		
C(6)−C(1)−O(1)−H(1)	−177.8(1)	−162.4(1)
C(2)−C(1)−O(1)−H(1)	2.0(1)	18.5(1)
C(2)−C(1)−C(6)−H(6)	−179.6(1)	177.9(1)
O(1)−C(1)−C(6)−C(5)	−179.8(1)	178.7(1)
C(2)−C(1)−C(6)−C(5)	0.4(1)	−2.1(1)
C(6)−C(1)−C(2)−H(2)	−179.8(1)	−178.5(1)
C(6)−C(1)−C(2)−C(3)	0.2(1)	1.5(1)
O(1)−C(1)−C(2)−H(2)	0.4(1)	0.7(1)
O(1)−C(1)−C(2)−C(3)	−179.6(1)	−179.3(1)
O(1)−C(1)−C(6)−H(6)	0.2(1)	−1.3(1)
C(1)−C(2)−C(3)−C(4)	−0.8(1)	0.4(1)
C(1)−C(2)−C(3)−H(3)	179.2(1)	−179.6(1)
H(2)−C(2)−C(3)−H(3)	−0.8(1)	0.4(1)
H(2)−C(2)−C(3)−C(4)	179.2(1)	−179.6(1)
C(2)−C(3)−C(4)−C(5)	0.9(1)	−1.7(1)
C(2)−C(3)−C(4)−N	−177.7(1)	178.2(1)
H(3)−C(3)−C(4)−N	2.3(1)	−1.8(1)
H(3)−C(3)−C(4)−C(5)	−179.1(1)	178.3(1)
C(3)−C(4)−N−O(2)	171.0(1)	179.1(1)
C(3)−C(4)−N−O(3)	−8.1(1)	−1.6(1)
C(3)−C(4)−C(5)−C(6)	−0.3(1)	1.1(1)
C(3)−C(4)−C(5−H(5)	179.7(1)	−178.9(1)
C(5)−C(4)−N−O(2)	−7.6(1)	−1.0(1)
C(5)−C(4)−N−O(3)	173.3(1)	178.3(1)
N−C(4)−C(5)−H(5)	−1.7(1)	1.2(1)
N−C(4)−C(5)−C(6)	178.3(1)	178.8(1)
C(4)−C(5)−C(6)−C(1)	−0.4(1)	0.8(1)
C(4)−C(5)−C(6)−H(6)	179.6(1)	−179.2(1)
H(5)−C(5)−C(6)−C(1)	179.6(1)	−179.2(1)
H(5)−C(5)−C(6)−H(6)	−0.4(1)	0.8(1)

density is commonly used.[24] Accordingly, the aspherical atomic density can be described in terms of spherical harmonics.

$$\rho_{atom}(r) = \rho_{core}(r) + \rho_{valence}(r) + \rho_{def}(r)$$

Thus for each atom,

$$\rho_{atom}(r) = \rho_{core}(r) + P_v\kappa^3\rho_{valence}(\kappa r) + \sum_{l=0}\kappa'^3 R_l(\kappa'\zeta r)\sum_{m=0}\sum_{p=\pm1} P_{lmp}\, y_{lmp}(\theta,\varphi)$$

with the origin at the atomic nucleus. The population coefficients, P_{lmp} are refined along with the κ and κ' parameters which control the radial dependence of the valence shell density. We have carried out a quantitative analysis of the electronic structure by using the critical point (CP) search developed by Bader and co-workers.[25] The set of CPs in $\rho(r)$ at r_c are defined such that $\nabla\rho(r_c) = 0$. The value of ρ_c in a bond measures its strength; the trace of the diagonalized Hessian at r_c (the Laplacian), $\nabla^2\rho_c$, measures the extent of depletion and contraction of charges, and the ellipticity ϵ, obtained as the ratios of the Hessian eigenvalues perpendicular to the bond minus 1, measures the degree of planarity or conjugation. The position of CP in a bond gives an idea of the polarity of the bond. The CP tends to shift closer toward the more electropositive atom and therefore the polarity of the bond, Δ, may be expressed as the percentage shift of the CP from the midpoint of the bond, normalized with half of the bond length. The vertical displacement, d, of CP from the line joining the bonded atoms measures the extent of bending of the bonding orbitals.

We shall first examine intramolecular bonding in the two modifications of *p*-nitrophenol. The residual density maps obtained as the difference between the calculated densities and the experimental densities were featureless, the magnitude of the random peaks being less than 0.12 e Å^{-3}. The static deformation density, $\Delta\rho$, was obtained as the difference between the total density and the spherical density without the thermal smearing, and the maps are shown in Figure 3 in the plane of the benzene ring. In both the β and α polymorphs, the deformation density builds up as concentric contours in the regions of the C−C bonds of the benzene ring, the C−N bond, the N−O bonds of the nitro group, and the C−O and the O−H bonds of the hydroxyl group. The lone-pair electrons of the oxygen atoms are also clearly seen in Figure 3. In order to be able to quantitatively compare the two charge densities in the polymorphs, we have carried out a critical point search along the different bonds. Regardless of the crystal form, the intramolecular CPs are of (+3,−1) type with negative Laplacians, characteristic of a covalently bonded molecular system.[25] In Table 3 we list the bond critical points of the β and α forms obtained from the present analysis.

The electron densities at the CPs, ρ_{CP}, of the six C−C bonds in the benzene ring vary in a rather narrow range, 2.2−2.35 e Å^{-3} for the β form and 2.01−2.20 e Å^{-3} for the α form, with mean values of 2.26 and 2.09 e Å^{-3}, respectively. The mean values of the Laplacians, $\nabla^2\rho_{CP}$, are −22.83 and −18.28 e Å^{-5}. Following Cremer and Kraka,[26] the ρ_{CP} and $\nabla^2\rho_{CP}$ values correspond to

(24) Hansen, N. K.; Coopens, P. *Acta Crystallogr.* **1978**, *A34*, 909.
(25) Bader, R. F. *Atoms in Molecules—a Quantum Theory*; International Series of Monographs in Chemistry 22; Oxford University Press: Oxford, U.K., 1990.
(26) Cremer, D.; Kraka, E. *Croat. Chem. Acta* **1984,** *57*, 1259.

Table 3. Analysis of the Bond Critical Points for the β (First Row) and α (Second Row) Forms[a]

bond	Hessian eigenvalues λ_1	λ_2	λ_3	ρ	$\nabla^2\rho$	ϵ	Δ%	d
O(1)−C(1)	−19.98	−19.19	19.14	2.32(6)	−20.0(3)	0.04	35.4 C(1)	0.022
	−17.56	−16.74	13.19	2.09(6)	−21.1(3)	0.05	22.9 C(1)	0.027
O(1)−H(1)	−44.40	−38.89	46.88	2.68(11)	−36.4(4)	0.14	47.7 H(1)	0.026
	−43.84	−40.31	38.94	2.91(6)	−45.2(6)	0.09	46.5 H(1)	0.041
O(2)−N	−27.45	−25.47	55.41	3.14(14)	2.5(4)	0.08	1.8 N	0.025
	−32.05	−28.02	51.38	3.49(8)	−8.7(3)	0.14	2.1 N	0.009
O(3)−N	−27.26	−21.86	59.72	3.03(2)	10.6(5)	0.25	0.6 N	0.031
	−31.10	−25.90	52.02	3.39(8)	−5.0(3)	0.20	0.6 O(3)	0.006
N−C(4)	−14.07	−11.77	13.29	1.91(5)	−12.5(2)	0.20	17.2 C(4)	0.018
	−13.76	−10.49	10.49	1.78(5)	−14.0(2)	0.29	25.5 C(4)	0.016
C(1)−C(2)	−17.71	−14.05	9.36	2.21(5)	−22.4(2)	0.26	5.6 C(2)	0.014
	−16.86	−13.33	12.11	2.08(5)	−18.1(1)	0.27	1.5 C(2)	0.011
C(1)−C(6)	−17.58	−14.47	9.71	2.27(6)	−22.3(2)	0.22	6.4 C(6)	0.013
	−16.50	−13.26	11.40	2.04(5)	−18.4(1)	0.24	6.4 C(6)	0.008
C(2)−C(3)	−17.20	−13.83	9.36	2.20(5)	−21.7(1)	0.24	4.0 C(2)	0.009
	−16.54	−13.54	12.05	2.09(5)	−18.0(1)	0.22	1.3 C(3)	0.005
C(2)−H(2)	−18.03	−17.28	18.70	1.89(5)	−16.6(2)	0.04	23.9 H(2)	0.015
	−17.78	−16.57	13.37	1.89(4)	−21.0(1)	0.07	20.0 H(2)	0.017
C(3)−C(4)	−16.85	−14.34	8.20	2.24(5)	−23.0(2)	0.18	12.7 C(3)	0.016
	−15.97	−13.20	11.39	2.01(5)	−17.8(1)	0.21	5.3 C(3)	0.012
C(3)−H(3)	−19.18	−17.15	17.32	2.01(4)	−19.0(2)	0.12	20.9 H(3)	0.015
	−19.01	−17.31	16.15	1.97(4)	−20.2(1)	0.10	24.6 H(3)	0.007
C(4)−C(5)	−18.08	−15.15	9.83	2.34(6)	−23.4(2)	0.19	5.1 C(5)	0.019
	−17.61	−14.46	12.72	2.20(5)	−19.4(1)	0.22	1.1 C(5)	0.014
C(5)−C(6)	−18.32	−15.60	9.76	2.35(6)	−24.2(2)	0.17	0.3 C(6)	0.018
	−16.26	−13.77	12.08	2.10(5)	−18.0(1)	0.18	3.9 C(5)	0.007
C(5)−H(5)	−18.65	−17.16	15.92	1.96(4)	−19.9(2)	0.09	18.5 H(5)	0.014
	−17.73	−16.81	14.20	1.97(4)	−20.3(1)	0.06	18.5 H(5)	0.007
C(6)−H(6)	−18.82	−16.45	15.69	1.96(4)	−19.6(2)	0.14	19.3 H(6)	0.015
	−16.91	−15.03	14.23	1.82(3)	−17.7(1)	0.13	20.0 H(6)	0.017

[a] ρ (e Å^{-3}) is the electron density, $\nabla^2\rho$ (e Å^{-5}) is the Laplacian, ϵ is the ellipticity, Δ is the bond polarity in percent, and d (Å) is the perpendicular distance between the critical point and the internuclear vector.

Table 4. Hydrogen Bond Critical Points[a]

bond	bond length	Hessian eigenvalues λ_1	λ_2	λ_3	ρ (e Å^{-3})	$\nabla^2\rho$ (e Å^{-5})	ϵ
			β Form[a]				
O(2)···H(2[a])	2.382(1)	−0.44	−0.27	1.80	0.076(14)	1.147(10)	0.65
O(3)··· H(1[a])	1.909(1)	−0.71	−0.45	5.82	0.11(3)	4.66(5)	0.58
O(1)···H(3[b])	2.345(1)	−0.25	−0.24	1.14	0.039(13)	0.66(1)	0.05
O(2)···H(5[c])	2.400(1)	−0.08	−0.05	0.38	0.007(8)	0.257(4)	0.65
			α Form[b]				
O(2)···H(1[a])	2.461(1)	−0.10	0.08	0.92	0.016(13)	0.897(8)	0.00
O(3)···H(1[a])	1.890(1)	−1.35	−1.11	4.89	0.19(3)	2.43(4)	0.23
N···H(1[a])	2.467(1)	−0.10	0.08	0.92	0.016(13)	0.897(8)	0.00
O(1)···H(2[b])	2.509(1)	−0.12	−0.06	0.99	0.029(9)	0.814(6)	0.98
O(3)···H(3[c])	2.617(1)	−0.13	−0.11	0.80	0.035(5)	0.562(2)	0.26
O(2)···H(5[d])	2.406(1)	−0.18	−0.12	1.19	0.040(10)	0.890(9)	0.48

[a] Symmetry codes: (a) $x - 1/2, -y + 1/2 + 1, z + 1/2$; (b) $-x + 1/2, y - 1/2, -x + 1/2 + 1$; (c) $-x - 1, -y + 1, -z + 2$. [b] Symmetry codes: (a) $x + 1, -y + 1/2, z + 1/2$; (b) $-x, y - 1/2, -z - 1/2$; (c) $-x + 1, -y + 1, -z$; (d) $-x + 2, -y, -z$.

Table 5. Pseudoatomic Charges and Dipole Moments

atom	β	α
O(1)	−0.09(9)	−0.29(10)
O(2)	−0.14(9)	−0.36(10)
O(3)	−0.22(9)	−0.30(10)
N	−0.47(21)	−0.60(22)
C(1)	0.00(13)	0.29(13)
C(2)	−0.01(12)	0.32(12)
C(3)	−0.08(13)	0.30(13)
C(4)	−0.49(13)	0.21(11)
C(5)	−0.06(12)	0.20(13)
C(6)	−0.10(12)	0.30(12)
H(1)	0.46(6)	0.03(11)
H(2)	0.32(7)	0.03(11)
H(3)	0.30(7)	−0.02(11)
H(5)	0.30(7)	−0.06(11)
H(6)	0.27(8)	0.02(10)
dipole moment (D)	21.5	18.0

mean bond orders of 2.02 and 1.70 in the β and the α forms, respectively, akin to those in aromatic rings. The ellipticity, ϵ, in both forms is somewhat lower than the theoretical value of 0.33. These homonuclear bonds are polarized little, some up to 12% due to perturbation caused by the two functional groups. The mean densities in the C−H bond regions of the benzene rings of the two forms are similar (∼1.9 e Å^{-3}) and are close to the theoretical density of 1.846 e Å^{-3}; the Laplacians are ∼−18.8 and −19.8 e Å^{-5} for the β and the α forms, respectively. The polarity of the C−H bonds, Δ, is expected to be 26.6% toward hydrogen, and we obtain mean Δ values close to 21% in the two forms.

The C(1)−O(1) bond connecting the hydroxyl group to the benzene ring is associated with ρ_{CP} values of 2.32 and 2.09 e Å^{-3} for the β and α forms, respectively. The corresponding bond orders are 1.43 and 1.23. The bond is polarized toward C(1), with Δ = 35.4% for the β modification (theoretical value ∼35%) and a lower value of 22.9% for the α modification. The O(1)−H(1) bond region also exhibits some differences. In this case, the

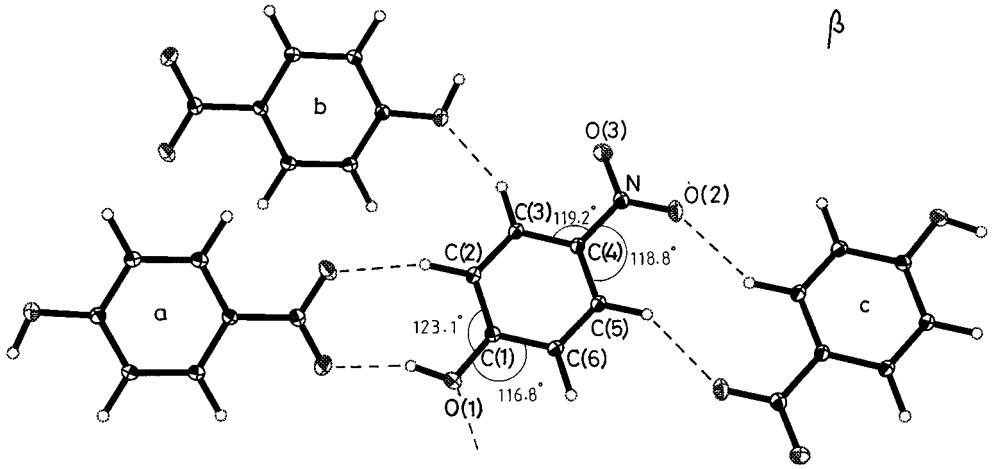

Figure 1. Molecular packing diagrams of the β polymorph of *p*-nitrophenol, showing 50% probability displacement ellipsoids.

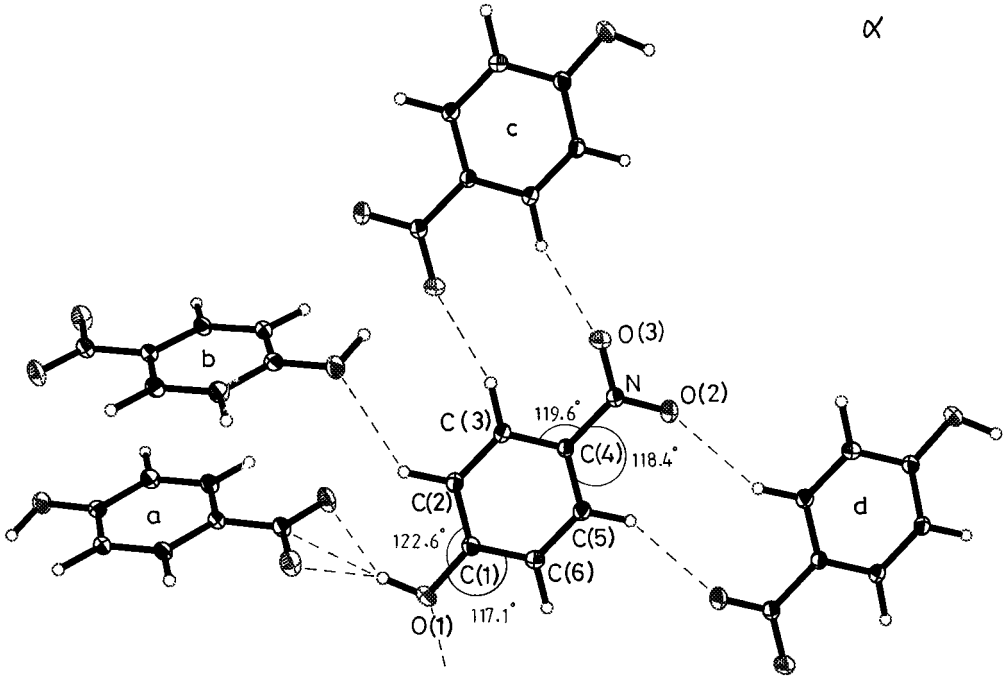

Figure 2. Molecular packing diagrams of the α polymorph of *p*-nitrophenol, showing 50% probability displacement ellipsoids.

ρ_{CP} value in the β form is lower than that in the in the α form by 0.23 e Å^{-3}. Interestingly, however, the CPs in the C(1)−O(1)−H(1) region deviate significantly ($d \sim 0.03$ Å) from the intermolecular vectors due to the bending of the orbitals (see Table 3), which is also reflected in the inequality of the C−C−O bond angles.

The C(4)−N bond linking the nitro group to the benzene ring is associated with ρ_{CP} values of 1.91 and 1.78 e Å^{-3} in the β and α forms, respectively, and with the corresponding bond orders of 1.03 and 0.93.[26] The bonding within the nitro group varies from one polymorph to the other and also between the two N−O bonds of the nitro group. The β form exhibits ρ_{CP} values of 3.14 and 3.03 e Å^{-3} for the N−O(2) and N−O(3) bonds, respectively, while the α form shows much higher densities of 3.49 and 3.39 e Å^{-3} for the same bonds, the latter being close to that expected for a double bond. The ellipticity of the N−O(3) bonds in both forms is somewhat larger than that of the N−O(2) bonds. The Laplacians and the bond polarities of N−O bonds are low in both forms, possibly because of the presence of the intermolecular hydrogen bonding.

From the above comparison of charge densities of the β and α forms, it appears that the density migrates outwardly from the benzene ring of the molecule to the nitro and the hydroxyl groups when the crystal structure changes from β to α. Accordingly, the group charges of NO_2 are −0.83 and −1.26 in the β and α forms, respectively, and the group charges of OH are +0.37 and −0.26, respectively. In Table 5 we list the pseudoatom charges in the two forms. The calculated molecular dipole moments in the two forms differ to some extent (Table 5), but both values are considerably larger than in the free molecule. The experimental values of the dipole moment of the free molecule[27] and that calculated by us[28] are around 5.5 D. This enhancement of the dipole moment clearly arises from the charge densities in the condensed state and is in line with that observed by Howard et al. for 2-methyl 4-nitroaniline.[17]

(27) Wesson, L. G. *Tables of Electric Dipole Moments*; MIT Press: Cambridge, MA, 1948.
(28) Stewart, J. J. P. MOPAC Program. *QChPE*, 1990.

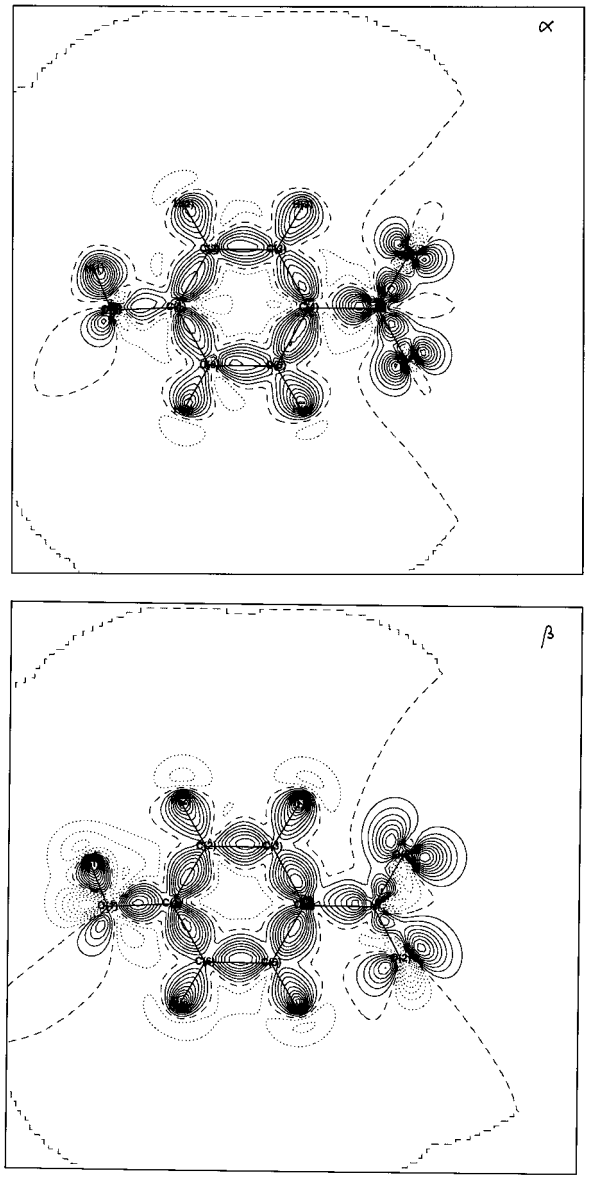

Figure 3. Static deformation density in the plane of the benzene ring for the β and the α forms of *p*-nitrophenol. Contour intervals at 0.1 e Å^{-3}.

The lone-pair electrons on the oxygen atoms of the nitro group occur as (+3,−3) critical points in the deformation density[13] and show significant differences between the two forms. The mean density of the lone-pairs is ∼5.5 e Å^{-3} in the β form, much smaller than that in the α form (∼7.6 e Å^{-3}).[6] We also notice that the lone-pair lobes are slightly closer to the nucleus in the α form (∼0.29 Å) as compared to the β form (∼0.39 Å).[13] Our later discussion of the intermolecular hydrogen bonding will bring this issue in the right perspective.

The hydrogen bonding between one of the oxygens of the nitro group and the hydroxyl hydrogen of the adjacent molecule (O(3)···H(1)) is the shortest intermolecular contact (∼1.9 Å) in both forms. Charge density analysis reveals the presence of bond critical points with small densities, 0.11 and 0.19 e Å^{-3} for the β and the α forms, respectively. The Laplacians at the CPs are also small and positive. These observations imply a closed shell interaction in the intermolecular hydrogen bonding.[26] Apart from the O(3)···H(1) contact, we have

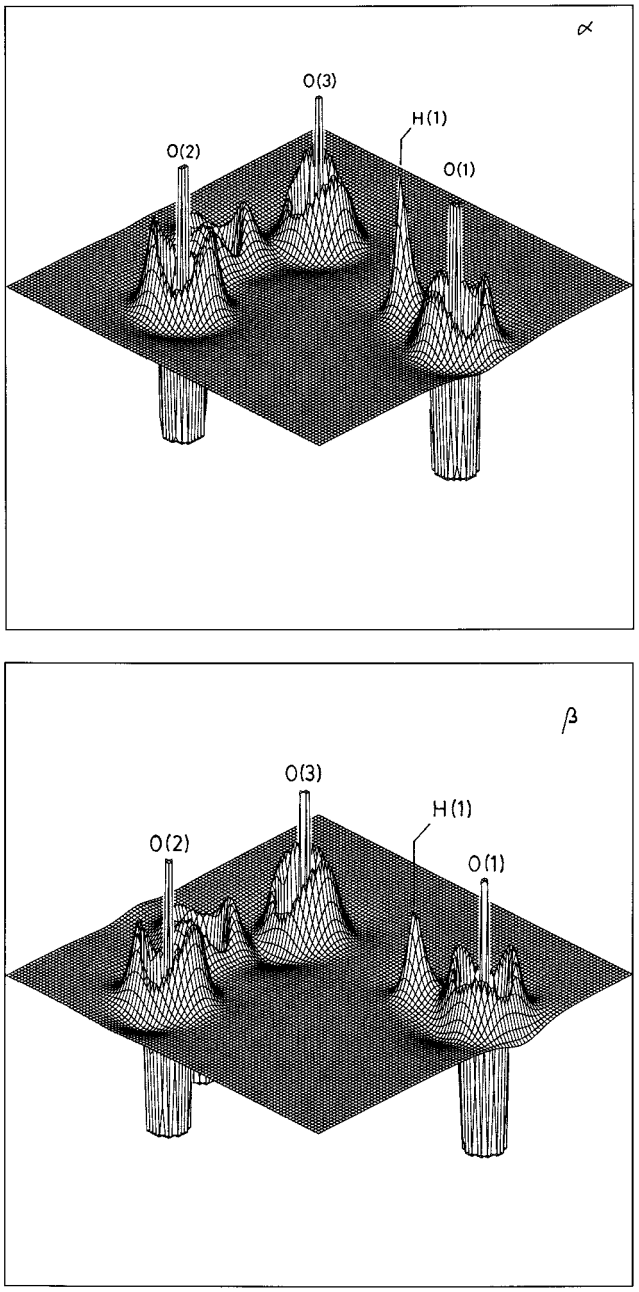

Figure 4. Relief maps of the negative Laplacian in the plane of the hydrogen bond (range, −250 to +250 e Å^{-5}) in the β and α forms of *p*-nitrophenol.

analyzed other hydrogen contacts as well. These are weak interactions as seen from the ρ_{CP} and $\nabla^2\rho$ values listed in Table 4. The two polymorphs exhibit some differences in the weak hydrogen bonds, the number of weak contacts being 5 and 8 in the β and α forms, respectively. The O(2)···H(2) contact in the β form is nearly parallel to the main hydrogen bond (see Figure 1) and exhibits a moderate density (0.076 e Å^{-3}) compared to the other weak contacts. An interesting feature in the α structure is that a common critical point is present with a density of ∼0.016 e Å^{-3} for the N···H(1) and O(2)···H(1) contacts, providing evidence for the participation of the entire nitro group in hydrogen bonding.

The variations observed in the intermolecular hydrogen bonding region involving the nitro group are best represented using relief maps of the negative Lapla-

cian.[6] We show such maps in Figure 4, for both polymorphs in the plane of the oxygen atoms of the nitro and the hydroxyl groups involved in the intermolecular bonding. We see from the figure that the oxygen lone-pair lobes are polarized in the direction of the hydrogen atom in both cases. A major difference between the two forms is that the hydroxyl group appears to have rotated and moved closer to the nitro group in the α form and that the hydrogen is now closer to the plane formed by the oxygen atoms, as seen from the increase in the intensity of the hydrogen peak in the map. The conclusions derived from the geometrical structure and the critical points of the intermolecular charge distribution are thus substantiated using the relief maps.

We carried out a preliminary study of the structure and charge distribution of red colored crystals obtained on irradiating the α form by visible light for several days. There were some definite changes in charge densities, and the calculated dipole moment was much smaller (14.5 D). Since we could not be certain of the nature of the reaction or its completion, we have not discussed the results here.

Conclusions

The present study on the β and α forms of *p*-nitrophenol demonstrates how significant differences in the structure, and in particular in the charge densities and related properties, can occur between the polymorphic forms of a molecular crystal, in the presence of intermolecular hydrogen bonding. The two polymorphs crystallize in the monoclinic system with similar densities (∼1.5 g/cm^3). While molecular geometry varies only slightly between the two forms, intermolecular hydrogen bonding differs considerably. The following are the main differences between the β and α forms:

(i) One of the oxygen atoms of the nitro group in the β form shows large displacement from the mean plane of the benzene ring (∼0.22 Å), while, in the α form, the hydroxyl hydrogen is maximally displaced (∼0.32 Å).

(ii) The two C−C−O bond angles differ by ∼6.24° in the β form and by a smaller value of ∼5.5° in the α form. One of the N−O bonds is larger by ∼0.01 Å in the α form.

(iii) The angle between the adjacent nonparallel molecules is ∼74.73° in the α form, and this value is much smaller (∼29.26°) in the β form.

(iv) The α form has a greater number of intermolecular hydrogen bonds compared to the β form. There are nine such contacts in the α form, while only six contacts are present in the β form. The strongest hydrogen bond originating from one of the oxygen atoms of the nitro group to the hydroxyl hydrogen is common to both forms.

(v) The charge densities at the critical points in the benzene ring and at the hydroxyl and the nitro linkages are noticeably larger in the β form than in the α form. The α form exhibits higher charge densities within the hydroxyl and the nitro groups. The Laplacians and the ellipticities of the various bonds are generally in good agreement with the theoritical predications.

(vi) The charge on the nitro group in the α form (∼−1.26) is much larger than in the β form (∼−0.83). The molecular dipole moments of the β and α forms are 21.5 and 18.0 D, respectively.

(vii) The lone-pair electrons on the oxygen atoms are closer to the nuclei (∼0.29 Å) in the α form than in the β form (∼0.39 Å). The mean densities are also higher in the α form.

(viii) The hydroxyl group in the α form is closer to the nitro group involved in intermolecular hydrogen bonding, and the entire nitro group participates in the hydrogen bonding unlike in the β structure, where the nitrooxygens involve phenyl hydrogens as well.

Acknowledgment. The authors thank the Department of Science and Technology, Government of India, for support of this research.

Supporting Information Available: Tables of atomic coordinates and anisotropic displacement parameters from high-order refinements, and population parameters obtained from multipole refinement (2 pages). Ordering information is given on any current masthead page.

CM980277M